

# Praseodymium-doped cubic Ca–ZrO<sub>2</sub> ceramic stain

J.A. Badenes\*, M. Llusar, M.A. Tena, J. Calbo, G. Monrós

*Inorganic Chemistry Area, Inorganic and Organic Department, Jaume I University, 12080 Castellón, Spain*

Received 10 January 2001; received in revised form 20 November 2001; accepted 2 December 2001

## Abstract

The cubic Ca–ZrO<sub>2</sub> structure has been used as host for preparing a yellow ceramic stain using praseodymium as dopant. Samples with Ca<sub>x</sub>Pr<sub>0.1</sub>Zr<sub>0.9-x</sub>O<sub>2</sub> ( $X=0.14, 0.17, 0.2$ ) compositions have been prepared by the ceramic method (CE) and by several gel processing techniques: the colloidal method (CG), the gelatine method (GE), the citrate method (CI) and a polymeric route (PG). Fired samples have been evaluated as ceramic pigments following enameling with the powders in ceramic glazes. The results show that a yellow ceramic pigment is obtained in all samples without significant differences among the different methods and compositions. This yellow ceramic pigment has been identified as a Pr–(Ca–ZrO<sub>2</sub>) solid solution. © 2002 Elsevier Science Ltd. All rights reserved.

*Keywords:* Pigments; (Pr,Ca,Zr)O<sub>2</sub>; Sol-gel processes; ZrO<sub>2</sub>

## 1. Introduction

Yellow is a particularly important colour in the ceramic pigment field. The consumption of yellow exceeds that of any other coloured pigment.<sup>1</sup> There are three important yellow pigment families: tin vanadia yellows (DCMA 11-22-4), praseodymium zircon (DCMA 14-43-4) and zirconia vanadia yellow (DCMA 1-01-4). Tin vanadia yellows<sup>2</sup> develop a strong yellow colour in all glazes, although the shade may be affected by the nature of the glaze. They are very opaque pigments. However, these pigments are sensitive to reducing conditions, and are incompatible with chromium-containing pigments. Praseodymium zircon pigments<sup>3</sup> have excellent tinting strength in most glazes. They can be used in most glazes, and are compatible with other pigments. Finally, in the V–ZrO<sub>2</sub> pigment, monoclinic zirconia gives a weaker yellow than tin vanadium and substantially muddier than praseodymium zircon yellows.<sup>4,5</sup>

Other yellow ceramic pigments commonly used such as Pb<sub>2</sub>Sb<sub>2</sub>O<sub>7</sub>, PbCrO<sub>4</sub> and CdS are now being expelled from the market because of their toxicity. Nowadays Pr–ZrSiO<sub>4</sub> yellow pigment has displaced V–SnO<sub>2</sub> and V–ZrO<sub>2</sub> yellows due to Pr–ZrSiO<sub>4</sub> being more intense

and more reproducible (in commercial conditions) than V–SnO<sub>2</sub> and V–ZrO<sub>2</sub>.

Reproducibility is an important commercial property for the pigments and it is very related to the mechanism of reaction involved in their production. A pigment, which the chromophore ion forms solid solutions with the host lattice, usually becomes more stable and more reproducible than inclusion or coating deposition of the chromophore on the substrate. For this reason, V–ZrO<sub>2</sub> and V–SnO<sub>2</sub> yellow pigments, in which V<sub>2</sub>O<sub>5</sub> is included or deposited on ZrO<sub>2</sub>(m)<sup>5</sup> and SnO<sub>2</sub><sup>6</sup> grains respectively, present reproducibility problems in industrial conditions. If novel yellow pigments are not obtained, the only yellow ceramic pigment in the future will be Pr–ZrSiO<sub>4</sub>. The research in the ceramic pigment field is consequently focused on two possible alternatives: to obtain a new host structure or to improve the colours already existing. The obtention of a yellow colour based on the solid solution mechanism will be an alternative to Pr–ZrSiO<sub>4</sub> in order to get more reproducible yellow colours.

Stabilized zirconias have been studied in recent decades because of their thermomechanical applications, such as thermal barrier coatings, oxygen sensors or toughened ceramics. The capacity of tetragonal zirconia and cubic zirconia polymorphs to achieve extended solid solutions with rare earth oxides makes them attractive for use in the ceramic pigment field as new host structures. In relation to this possibility, studies of

\* Corresponding author.

*E-mail address:* jbadenes@qio.uji.es (J.A. Badenes).

the synthesis of the Pr–ZrSiO<sub>4</sub> pigment by sol-gel routes<sup>7</sup> have shown a new yellow colour, associated with tetragonal zirconia, obtained from these non-conventional methods.

On the other hand, recent works<sup>8</sup> have shown that Pr<sub>6</sub>O<sub>11</sub> does not stabilise the *t* or *c* zirconia polymorphs. However, CaO exhibits extended solubility in ZrO<sub>2</sub> producing oxygen vacancies which can increase the praseodymium solubility in the zirconia lattice as with others cations.<sup>9</sup> Therefore, if the solid solution obtained withstands the action of an enamel matrix at the enameling temperature without solubilization and with colouring intensity like that of V–ZrO<sub>2</sub>, it would be a valid new alternative yellow pigment.

The aim of this work is to obtain a pigment using stabilized Ca–ZrO<sub>2</sub> as host structure and praseodymium as dopant and to test its stability in conventional ceramic glazes.

One further objective is to analyse the effect of the reactivity of the starting powders on the pigment synthesis. The reactivity of powders has been modified using different synthesis routes: ceramic (CE) and sol-gel routes. Several sol-gel routes have been used such as the colloidal (CG), gelatine (GE), citrate (CI) and polymeric from alcoxides (PG) routes.

## 2. Experimental procedure

According to the phase diagram of the ZrO<sub>2</sub>–CaO system,<sup>10</sup> a metastable cubic solid solution region exists below the eutectoid point at 1140 °C and 17% molar CaO composition. In order to study the effect of doping with Pr<sub>2</sub>O<sub>3</sub>, three compositions have been chosen: a molar ratio in ZrO<sub>2</sub>–CaO on the ZrO<sub>2</sub>-rich side of the above mentioned region (composition 1), within the region (composition 2) and on the CaO-rich side of the region (composition 3). This design of sample compositions makes it possible to get metastable cubic zirconia at least in the sample with composition 2 firing at 1100 °C, in accordance with the phase diagram. The three different compositions are shown in Table 1.

Four gel methods for each composition have been prepared: the colloidal gel method (CG), the gelatine protected gel method (GE), the citrate method (CI) and the polymeric gel method (PG). Using a conventional ceramic method, composition 3 has been prepared as reference in order to compare with the products of the

gel methods and to check the quality of pigment produced by this method. Flow diagrams for gel methods are shown in Fig. 1. The raw materials used in the synthesis are given in Table 2.

The precursors in the ceramic method (CE) were ball-milled in acetone for 20 min. Residual acetone was then removed by evaporation, and the resulting dried powder was finally homogenized in an agate mortar.

In the colloidal gel method (CG), soluble salts of Zr, Ca, and Pr (Table 2) were solved in 250 ml of water at 70 °C with continuous stirring in amounts equivalent to 10 g of final composition (Table 1). Then, concentrated

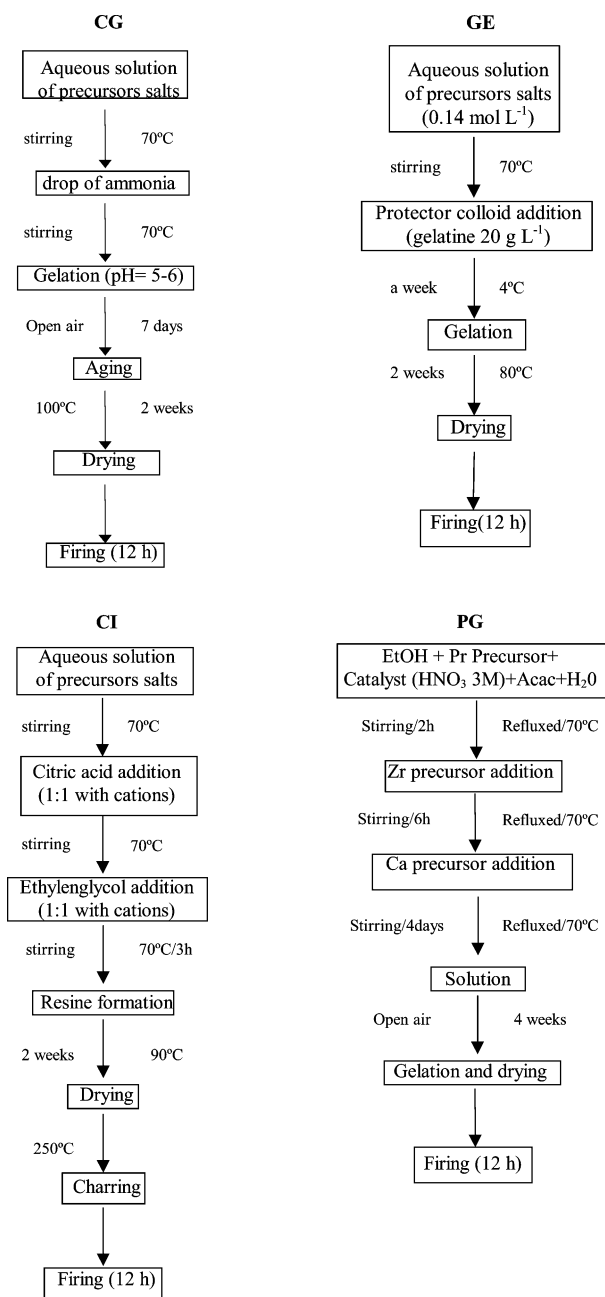


Fig. 1. Flow diagrams for the colloidal (CG), gelatine (GE), citrate (CI) and polymeric routes (PG).

Table 1  
Molar composition of samples

Composition	ZrO <sub>2</sub>	CaO	Pr <sub>2</sub> O <sub>3</sub>
1	76	14	5
2	73	17	5
3	70	20	5

Table 2  
Raw materials

Method	Precursors
CE	ZrO <sub>2</sub> (baddeleyite), CaCO <sub>3</sub> (PANREAC), Pr <sub>6</sub> O <sub>11</sub> (Rhône Poulenc)
CG	ZrOCl <sub>2</sub> ·8H <sub>2</sub> O (Merck), Ca(CH <sub>3</sub> COO) <sub>2</sub> ·H <sub>2</sub> O (PANREAC) Pr(CH <sub>3</sub> COO) <sub>3</sub> ·3H <sub>2</sub> O (Johnson Matthey), NH <sub>3</sub> <sup>a</sup>
GE	ZrOCl <sub>2</sub> ·8H <sub>2</sub> O (Merck), Ca(CH <sub>3</sub> COO) <sub>2</sub> ·H <sub>2</sub> O (PANREAC) Pr(CH <sub>3</sub> COO) <sub>3</sub> ·3H <sub>2</sub> O (Johnson Matthey) <sup>b</sup>
CI	ZrOCl <sub>2</sub> ·8H <sub>2</sub> O (Merck), Ca(CH <sub>3</sub> COO) <sub>2</sub> ·H <sub>2</sub> O (PANREAC) Pr(CH <sub>3</sub> COO) <sub>3</sub> ·3H <sub>2</sub> O (Johnson Matthey) <sup>c</sup>
PG	C <sub>12</sub> H <sub>28</sub> O <sub>4</sub> Zr (Fluka), CaCl <sub>2</sub> (PANREAC) Pr(CH <sub>3</sub> COO) <sub>3</sub> ·3H <sub>2</sub> O (Johnson Matthey).

<sup>a</sup> Agent of precipitation.

<sup>b</sup> Gelatine from Panreac.

<sup>c</sup> Citric acid from Panreac.

ammonia water solution was dropped until gelation occurred at pH = 5–6. This gel was aged at room temperature in the open air and dried at 100 °C. Then it was crushed and ground in an agate mortar.

The starting inorganic salts were dissolved in water with a concentration of 0.14 mol/l for the metallic cations in the protected gel route<sup>11</sup>(GE). Gelatine (5.94 g) previously swollen by immersion in water, was dissolved in 300 ml of hot water to give a transparent colloidal solution. This solution was added to the solution of inorganic salts and stirred at 70 °C to give a transparent solution. It was kept at 4 °C for 1 week to give a homogenous and transparent gel. The obtained gel was dried at 80 °C.

In the citrate method (CI), ZrOCl<sub>2</sub>·8H<sub>2</sub>O, calcium acetate and praseodymium (III) acetate were dissolved in the same conditions as above for the colloidal method. The metallic solution was complexed by addition of citric acid and continuous stirring at 70 °C using as molar ratio metallic cations: citric acid = 1:1. The resulting solution was esterified with ethylenglicol using as molar ratio, metallic cations: ethylenglicol = 1:1. The new solution obtained was heated, with stirring, up to 70 °C for 3 h in order to promote the polyesterification. The polyester was dried at 90 °C and submitted to a charring treatment at 250 °C to eliminate organics.

Ethanol was used in the polymeric gel method as the solvent media. Firstly, the precursor of praseodymium, the acid catalyst (3 M HNO<sub>3</sub>), acetylacetone and water (keeping the molar ratios shown in Table 3) were refluxed with continuous stirring at 70 °C for 2 h in ethanol media. Then, zirconium (IV) propoxide was added to the solution and hydrolysed for 6 h, maintaining the same reflux conditions. Finally, calcium precursor was added and the sample was continuously stirred at 70 °C for 4 days. The gelation and drying were performed at room temperature in the open air 4 weeks later.

Differential thermal analysis (DTA) and thermogravimetric analysis (TG), were carried out using a Perkin-Elmer instrument in air with a platinum crucible and with heating at 10 °C/min. Powdered alumina was used as reference.

Samples were fired at temperatures of 500, 900 and 1100 °C successively with 12 h soaking time. In order to obtain cubic stabilized zirconia in the ceramic method, the material was fired at 1200 and 1400 °C with the same soaking time.

XRD powder diffractograms were obtained using a Philips X-ray diffractometer using nickel filtered CuK<sub>α</sub> radiation (0.05°2θ s<sup>-1</sup> and 1 s of counting time per step). Operating at lower goniometer speed (0.02°2θ s<sup>-1</sup>), the crystallite size and the concentration of tetragonal zirconia were calculated. The crystallite size was obtained using the Scherrer's relationship.<sup>12</sup> The relative zirconia concentration was evaluated by direct X-ray counts corresponding to *hkl* = 111 area. Zirconia cell parameters were measured using α-Al<sub>2</sub>O<sub>3</sub> as internal standard by the POWCAL and LSQC calculation programmes.<sup>13</sup>

UV-visible (UV-V) spectra were obtained in the range between 200 and 1600 nm, by the diffuse reflectance method on a Lamda 19 spectrophotometer manufactured by Perkin Elmer. CIE-*L\*a\*b\** values [parameters of colour evaluation of Comission International de l'Eclairage<sup>14</sup>: *L\** (lightness axis), *a\** (green → red axis) and *b\** (blue → yellow axis)], were measured using the standard lighting C. Similarly, the *x-y* CIE chromatic parameters, that make it possible to obtain the dominant reflected wavenumber  $\lambda$ , were measured.

Microstructural analysis by SEM-EDX (scanning electron microscope-energy dispersion X-ray) was carried out in a LEICA LEO440I equipped with an Oxford LYNK EDX system.

Table 3  
Molar ratio conditions in polymeric route<sup>a</sup>

	Molar ratio
Zr(OPr) <sub>4</sub> :ethanol	1:26
Zr(OPr) <sub>4</sub> :acac	1:1
Zr(OPr) <sub>4</sub> :H <sub>2</sub> O	1:3
Zr(OPr) <sub>4</sub> :H <sup>+</sup>	1:0.18

<sup>a</sup> acac: Acetylacetone; Zr(OPr)<sub>4</sub>: zirconium (IV) propoxide.

### 3. Results and discussion

DTA and TG curves of representative raw samples are shown in Fig. 2. In all gel methods the DTA curves display common features.

(i) The DTA curves exhibit two endothermic peaks at 120–250 °C associated with a weight loss in the TG curves, which could be ascribed to the evaporation of residual water and chloride entrapped in the gel.

(ii) In the temperature range 300–500 °C, two exothermic peaks are observed. Also in this temperature region, the TGA shows a weight loss in all samples,

indicating that it can be ascribed to the oxidation of organics (about 300 °C) and to the decomposition of acetate groups (about 500 °C).

The exothermic peak around 700 °C, clearly observed in the DTA curve of the CG3 sample (Fig. 2), without a corresponding loss in weight, is associated with zirconia crystallization, the only crystalline phase detected by XRD of the resulting powder. All samples become yellow coloured.

The evolution of the crystalline phases detected and the colour of samples as a function of firing temperature are summarized in Table 4. Representative XRD diffractograms are shown in Fig. 3.

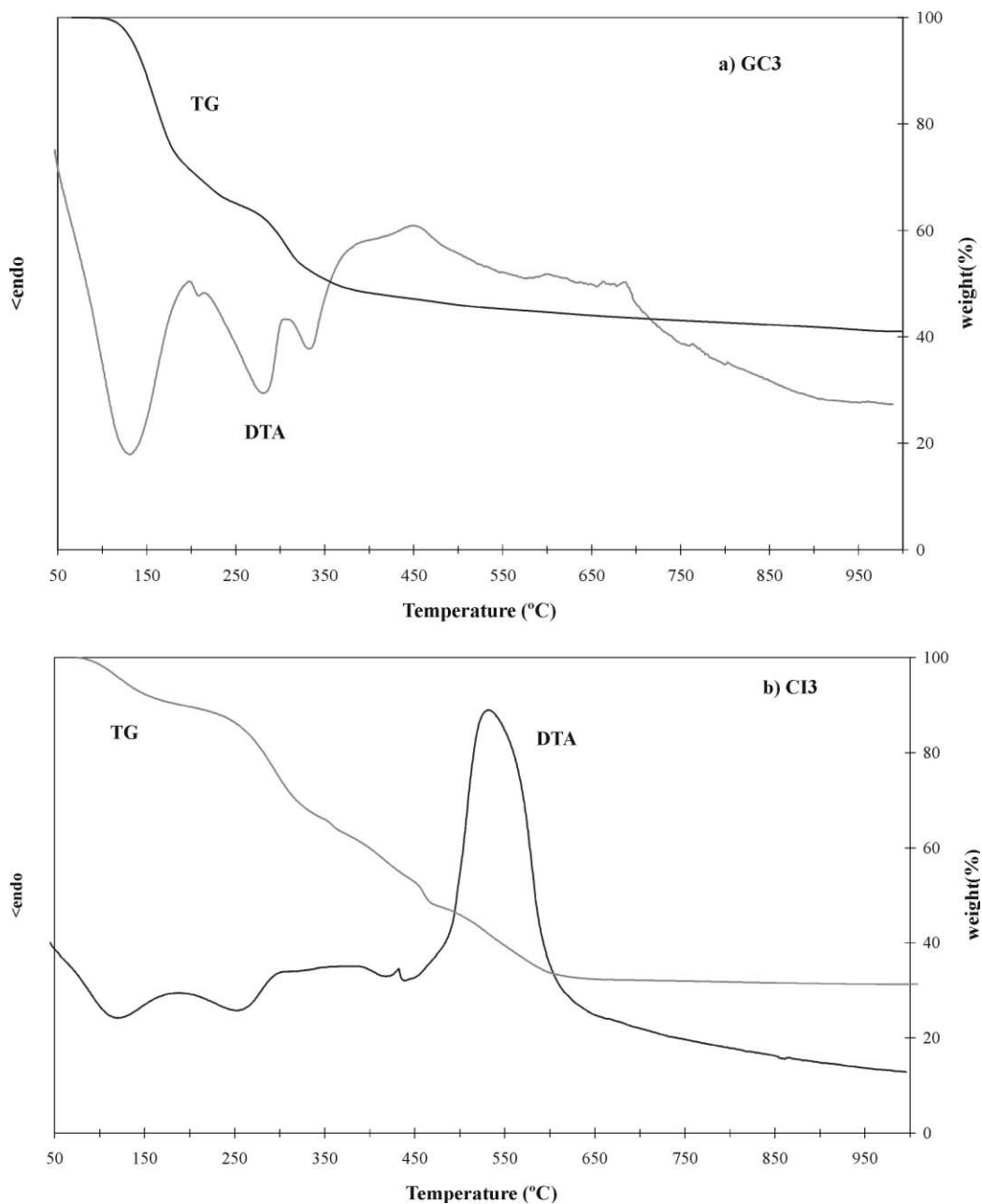


Fig. 2. DTA and TG curves of samples. (a) sample CI3 (citrate route with composition 3:  $\text{Ca}_{0.2}\text{Pr}_{0.1}\text{Zr}_{0.70}\text{O}_2$ ). (b) sample CG3 (colloidal gel route with composition 3:  $\text{Ca}_{0.2}\text{Pr}_{0.1}\text{Zr}_{0.70}\text{O}_2$ ).

The raw samples prepared by the sol-gel methods, with a green colour, are amorphous to XRD; however, in the CG samples, weak intensity peaks are detected which are assigned to the  $\text{NH}_4\text{Cl}$  crystalline phase. The gelatine, citrate and colloidal samples fired at 500 °C present wide XRD peaks of very weak intensity associated to  $\text{ZrO}_2$  (*t*) and they become yellow. The crystallization of this metastable  $\text{ZrO}_2$  indicates the high reactivity of those synthesis methods, probably associated with a heterogeneous nucleation mechanism. However, PG samples fired at 500 °C are black due to trapped unoxidized carbon particles and they remain amorphous. This is due to the high homogeneity of the starting gel, which makes it likely that the crystallization occurs by homogeneous nucleation mechanism delaying the growth of crystallites.<sup>15</sup>

All gel samples fired at 900 °C present wide XRD peaks of medium intensity associated with tetragonal zirconia and yellow colour (Table 4).

At 1100 °C metastable cubic  $\text{ZrO}_2$  is found in all gel samples, with  $\text{CaZrO}_3$  in the citrate and gelatine routes of the richest calcium samples. The yellow colour is maintained. The citrate method presents the strongest intensity peaks associated with  $\text{ZrO}_2$  (*c*) and  $\text{CaZrO}_3$  (Fig. 3).

For each method, there are not differences between the different compositions, except in the gelatine and citrate routes where  $\text{CaZrO}_3$  is detected only in composition 3 (GE3 and CI3).

The ceramic sample (CE3) presents different reactivity than the samples prepared by the sol-gel methods. Precursors are unreacted until 500 °C. At 900 °C  $\text{CaZrO}_3$  is detected and this phase remains during all heat treatments (1400 °C). Pyrochlore ( $\text{Pr}_2\text{Zr}_2\text{O}_7$ ), not detected in the gel samples, is observed from 1100 to 1200 °C

(Table 4) and only when this phase is destabilized at 1400 °C, does metastable  $\text{ZrO}_2$  (*c*) become the main phase and the colour become yellow.

The percentage of zirconia and the crystallite size of the fired samples is studied in the gel samples because of the different reactivity in relation to the ceramic sample above mentioned (Table 4). The results are given in Table 5.

At 900 °C the citrate route presents the highest percentages of metastable  $\text{ZrO}_2$  for each composition and the PG samples always present a lower zirconia concentration due to its homogeneous mechanism of nucleation.<sup>15</sup>

The observed broad XRD peaks at 900 °C (Fig. 3), indicative of small crystallite size, hinder the clear identification of metastable cubic or tetragonal zirconia, which may show similar X-ray diffraction patterns<sup>16,17</sup> under these conditions. However, it is well known in the literature that metastable tetragonal zirconia crystallizes from amorphous zirconia and it destabilizes when the size grows past 30 nm.<sup>18</sup> Because of that, in accordance to the crystallite size measured in the samples and shown in Table 5, the zirconia crystallized at 900 °C has been assigned to tetragonal zirconia (size < 30 nm). On the other hand, the clear and strong XRD zirconia peaks at 1100 °C shown in Fig. 3 (without characteristic doublet tetragonal peaks<sup>17</sup>) and with a crystallite size bigger than 30 nm has been XRD indexed as stabilized cubic zirconia polymorph.

Measurements of cubic zirconia crystallographic parameters by POWCAL and LSQC programmes are given in Table 6. The cell parameters of  $\text{ZrO}_2$ –CaO without praseodymium are in agreement with literature data.<sup>19</sup> An increase in  $\text{ZrO}_2$ –CaO solid lattice parameters must be expected if praseodymium enters solution because the ionic radius of the dopant as proposed by

Table 4  
Crystalline phases and colour of samples

Method composition	RAW	500 °C	900 °C	1100 °C
CG1	N(w)gr	T(w)ye	T(m)ye	C(s)ye
CG2	N(w)gr	T(w)ye	T(m)ye	C(s)ye
CG3	N(w)gr	T(w)ye	T(m)ye	C(s)ye
CI1	Agr	T(w)ye	T(m)ye	C(vs)ye
CI2	Agr	T(w)ye	T(m)ye	C(vs)ye
CI3	Agr	T(w)ye	T(m)ye	C(vs)Z(w)ye
GE1	Agr	T(w)ye	T(m)ye	C(vs)ye
GE2	Agr	T(w)ye	T(m)ye	C(vs)ye
GE3	Agr	T(w)ye	T(m)ye	C(vs)Z(vw)ye
PG1	Agr	Abk	T(m)ye	C(s)ye
PG2	Agr	Abk	T(m)ye	C(s)ye
PG3	Agr	Abk	T(m)ye	C(vs)ye
	900 °C	1100 °C	1200 °C	1400 °C
CE3	M(s) Z(m) Pr (vw) gray	M(s), Z(m) Py(vw) gray	M(m) Z(m) Py(w),C(vw) gray	C(vs), Z(md) M(vw) yellow

Peak intensity: vs (very strong), s (strong), m (medium), w (weak), vw (very weak).

Crystalline phases: A (amorphous), N ( $\text{NH}_4\text{Cl}$ ), T ( $\text{ZrO}_2$  tetragonal), C ( $\text{ZrO}_2$  cubic), Z ( $\text{CaZrO}_3$ ), Ca ( $\text{CaCO}_3$ ), Py ( $\text{Pr}_2\text{Zr}_2\text{O}_7$ ).

Colour: gr (green), br (brown), ye (yellow), bk (black).

CG (colloidal gel), GE (gelatine), CI (citrate), PG (polymeric gel).

Composition: 1 (composition  $\text{Ca}_{0.14}\text{Pr}_{0.1}\text{Zr}_{0.76}\text{O}_2$ ), 2 (composition  $\text{Ca}_{0.17}\text{Pr}_{0.1}\text{Zr}_{0.73}\text{O}_2$ ), 3 (composition  $\text{Ca}_{0.2}\text{Pr}_{0.1}\text{Zr}_{0.7}\text{O}_2$ ).

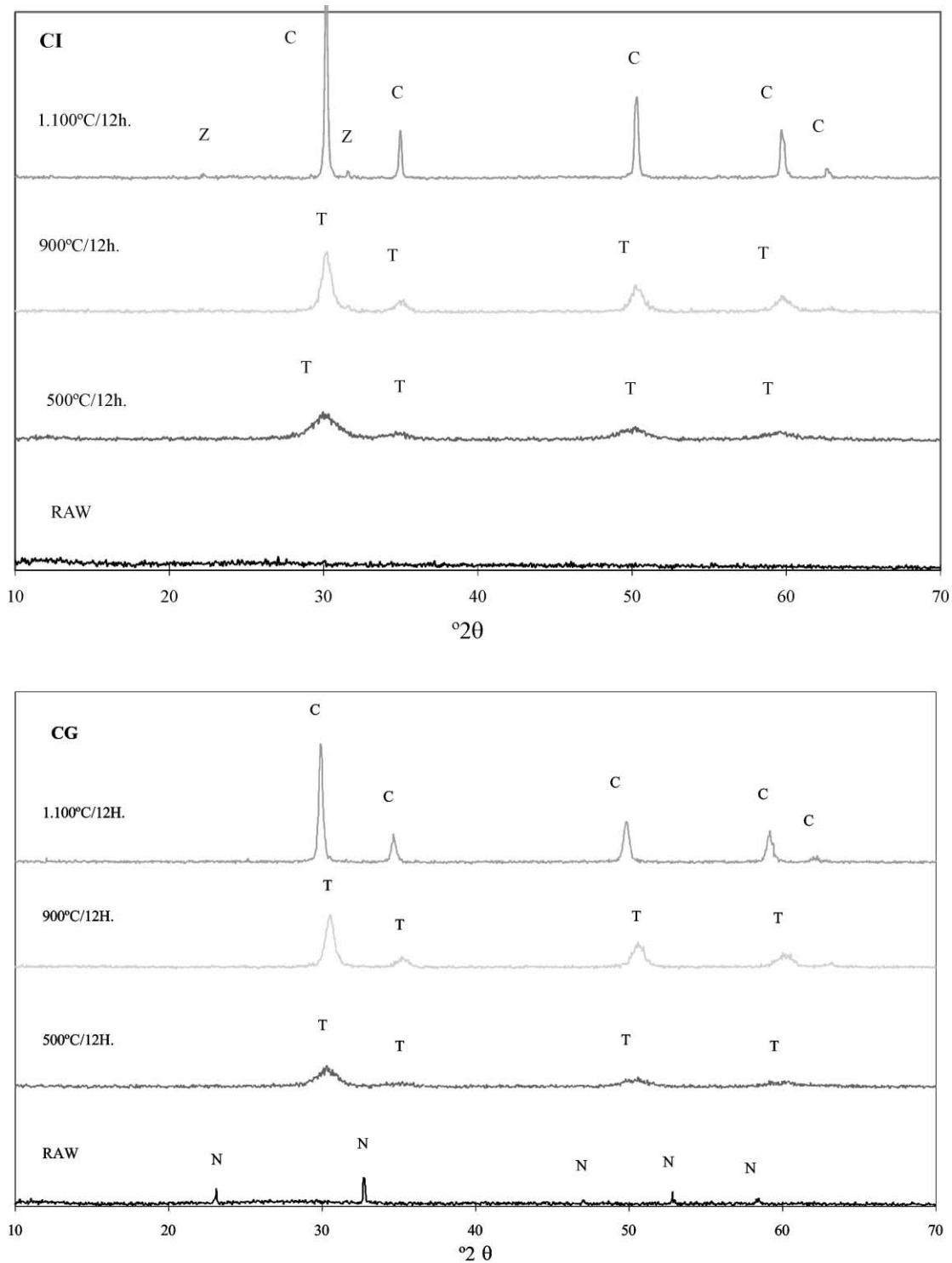


Fig. 3. Evolution of XRD for colloidal (CG) and citrate (CI) route with composition 3 ( $\text{Ca}_{0.2}\text{Pr}_{0.1}\text{Zr}_{0.70}\text{O}_2$ ) as a function of firing temperature. Crystalline phases: T,  $\text{ZrO}_2$  (t); C,  $\text{ZrO}_2$  (c), Z,  $\text{CaZrO}_3$ .

Shanon<sup>20</sup> ( $\text{Pr}^{3+} = 1.14 \text{ \AA}$  or  $\text{Pr}^{4+} = 0.99 \text{ \AA}$ ) is bigger than that of  $\text{Zr}^{4+} = 0.84$  (all for 8-fold coordination). Therefore, the results in Table 6 indicate the entrance of praseodymium into solid solution in the  $\text{ZrO}_2$ – $\text{CaO}$  lattice.

In order to evaluate the interest of the obtained yellow samples, the powder was evaluated by UV–V spectroscopy

(Fig. 4) and enamelled in a transparent glaze by adding 5 and 20% of pigment and firing at 1000 °C/1 h on a ceramic support. CIE- $L^*a^*b^*$  measurements were carried out on samples fired at 1100 (1400 °C in the case of the ceramic sample) and on the 5% enamel samples (Table 7). The 20% enamel sample was characterized by XRD (Fig. 5).

Table 5  
Percentage of zirconia and crystallite size in fired samples

Method	Composition	% (ZrO <sub>2</sub> )		Crystallite size (nm)	
		900 °C	1100 °C	900 °C	1100 °C
CG	1	88	–	22	–
	2	74	–	21	–
	3	85	100	22	51
GE	1	69	–	24	–
	2	74	–	25	–
	3	83	98	27	54
CI	1	100	–	24	–
	2	95	–	25	–
	3	85	99	26	57
PG	1	79	–	24	–
	2	63	–	22	–
	3	80	86	22	54

Table 6  
Zirconia cell parameters of cubic zirconia in samples fired at 1100 °C. (Values in parenthesis are the estimated standard deviation)

Method (composition 3)	a = b = c (Å)	V (Å <sup>3</sup> )
Zirconia blank <sup>a</sup>	5.127(2)	134.7(2)
CG	5.177(1)	138.75(4)
CI	5.185(1)	139.39(8)
GE	5.189(2)	139.7(2)
PG	5.183(1)	139.23(8)

<sup>a</sup> Ca–ZrO<sub>2</sub> sample without praseodymium doping prepared by the colloidal gel method.

The UV-V spectra of the yellow samples present similar features in all samples and compositions: two weak bands at 225, 270 nm and a sharp band at 300 nm in the UV region, a shoulder around 400 nm and three IR bands at 1020 (very weak), 1450 and 1525 nm respectively. The sharp band at 300 nm is associated with the calcium stabilizer in the zirconia<sup>21</sup> but it is dif-

Table 7  
CIE-*L\*a\*b\** colorimetric parameters of samples fired at 1100 °C and enamel samples in transparent glaze with 5% of pigment

Sample	<i>L*</i>	<i>a*</i>	<i>b*</i>	<i>x</i>	<i>y</i>	λ (nm)
CE3*	80	3.5	23.2	0.376	0.387	576
GE1	82	1.9	19.7	0.356	0.370	576
GE2	79	3.5	23.0	0.367	0.370	577
GE3	76	4.0	23.6	0.370	0.380	575
CI1	84	3.5	22.9	0.363	0.374	576
CI3	72	6.0	24.0	0.377	0.379	578
CG3	72	5.6	23.0	0.377	0.377	578
PG1	82	1.5	21.4	0.358	0.374	575
PG3	74	4.9	24.0	0.375	0.378	578
<i>Enameled</i>						
PG1	86.17	−2.96	26.08	0.359	0.385	574
GE3	86.84	−3.19	24.92	0.355	0.383	574

PG: polymeric gel ; GE: gelatine protected gel; CG: colloidal gel; CI: citrate gel; CE\*: ceramic sample fired at 1400 °C/12 h.1: composition Ca<sub>0.14</sub>Pr<sub>0.1</sub>Zr<sub>0.76</sub>O<sub>2</sub>; 2: composition Ca<sub>0.17</sub>Pr<sub>0.1</sub>Zr<sub>0.73</sub>O<sub>2</sub>; 3: composition: Ca<sub>0.20</sub>Pr<sub>0.1</sub>Zr<sub>0.70</sub>O<sub>2</sub>.

icult to assign the rest of spectra. Characteristic bands of Pr<sup>3+</sup> (441, 464, 488 and 590 nm)<sup>22</sup> are not clearly observed and the praseodymium valence cannot be decided from the spectra data. The intensity of the shoulder is the main characteristic to improve the yellow colour of the sample and it is similar in all samples. In Fig. 4 are represented the lowest and the highest shoulder intensity obtained in the samples. The level of the absorbance indicates that the yellow intensity of the obtained colour corresponds to a soft yellow colour.

The CIE-*L\*a\*b\** measurements summarized in Table 7 show that a yellow colour is obtained in all samples (high *b\** and low *a\** parameters) and a light colour (*L\** by 80) in agreement to the UV-V spectra. The richest calcium samples present higher *b\** and *a\** parameters (more yellow intensity but with reddish shades) and lightness. The *x,y* measurements recorded

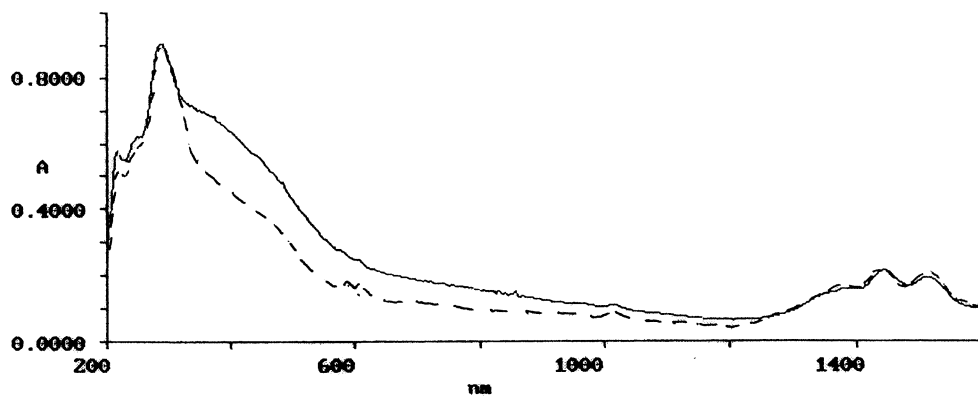


Fig. 4. UV-V spectra of samples fired at 1100 °C: (—) PG3 (polymeric gel with composition 3: Ca<sub>0.2</sub>Pr<sub>0.1</sub>Zr<sub>0.70</sub>O<sub>2</sub>), (---) PG1 (polymeric gel with composition 1: Ca<sub>0.14</sub>Pr<sub>0.1</sub>Zr<sub>0.76</sub>O<sub>2</sub>).

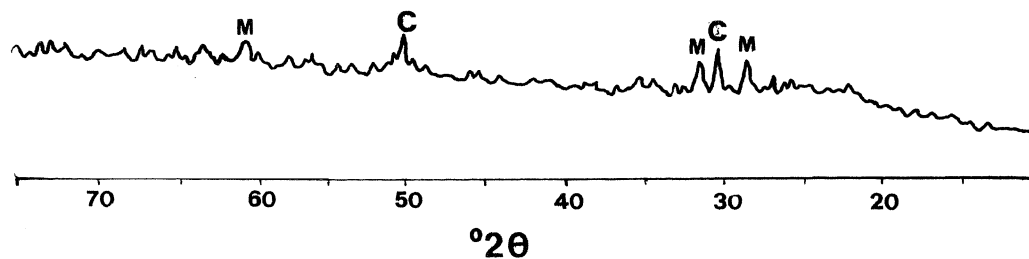


Fig. 5. XRD of enameled in transparent glaze (GE1 gelatine route with composition 1:  $\text{Ca}_{0.14}\text{Pr}_{0.1}\text{Zr}_{0.76}\text{O}_2$ , fired  $1100^\circ\text{C}$ ): with 20% colour fired at  $1000^\circ\text{C}/1\text{ h}$ . Crystalline phases: C,  $\text{ZrO}_2$  (c); M,  $\text{ZrO}_2$  (m).

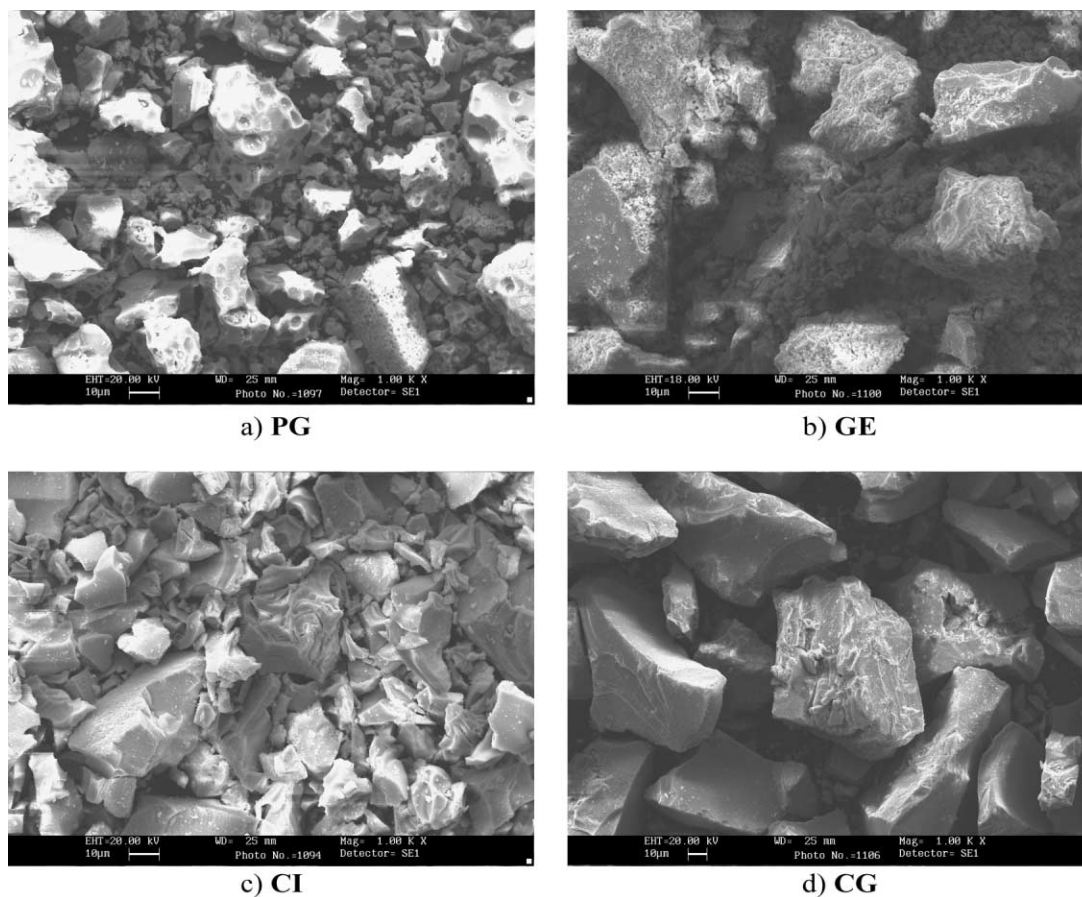


Fig. 6. SEM Micrographs of richest calcium samples fired at  $1100^\circ\text{C}/12\text{ h}$ : (a) PG (polymeric gel), (b) GE (gelatine gel), (c) CI (citrates gel), (d) CG (colloidal gel).

in Table 7 indicate that the dominant reflected wavelength is around 577 nm in powered samples and 574 nm in enameled samples.

The XRD of the 20% enamel sample (Fig. 5) indicates that cubic metastable zirconia phases remain in the enamel sample but that the monoclinic polymorph is also detected indicating that glaze interaction partially destabilizes the cubic zirconia.

The microstructure of representative samples fired at  $1100^\circ\text{C}/12\text{ h}$  is reported in Fig. 6. The synthesis method influences the microstructure: zirconia appears agglom-

erate in all samples but the polymeric samples (PG) present the lowest values of aggregate size (1–30  $\mu\text{m}$ ); gelatine (GE) and citrate (CI) route samples present aggregates between 10 and 40  $\mu\text{m}$  and the colloidal sample (CG) shows (Fig. 6d) the biggest agglomerate size (30–70  $\mu\text{m}$ ). In the PG (Fig. 6a) samples a superficial porosity due to elimination of the *n*-propoxide precursor of zirconium. The particle size is not distinguished except in the gelatine route (Fig. 6b) where agglomerates are formed by nanometric spherical particles of 200–500 nm.



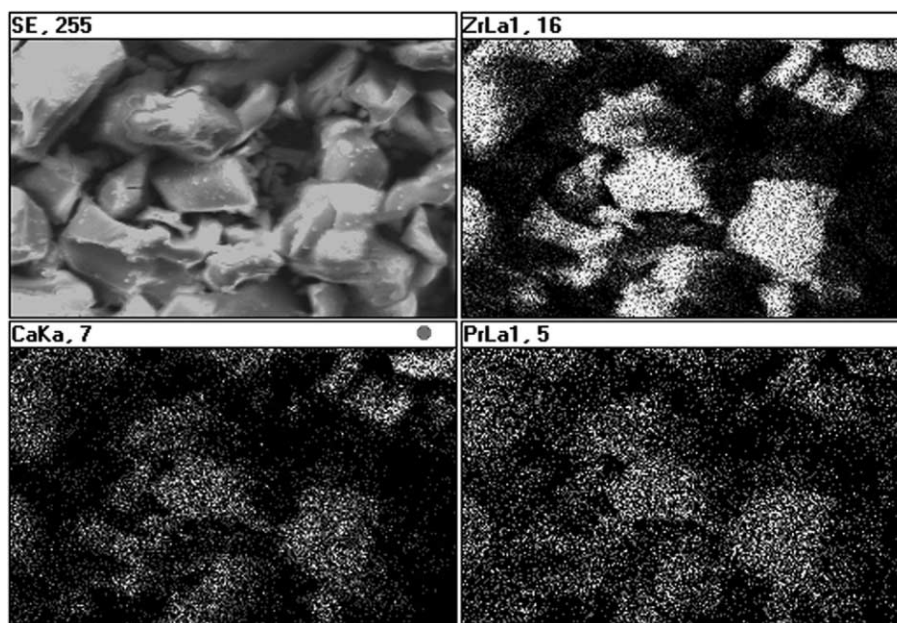


Fig. 7. Mapping of richest calcium sample fired at 1100 °C prepared by citrates method (CI3).

The mapping analysis of a representative sample is given in Fig. 7. Samples present an homogeneous distribution of Ca, Zr and Pr, and EDX analysis (not shown) is in agreement with the theoretical composition. The homogeneous distribution of praseodymium in the sample confirms the Pr solid solution as discussed.

The results show that a yellow ceramic pigment is obtained in all samples without significant differences among different methods. The solid solution nature of this pigment is in agreement with these results. The influence of the microstructure is not so decisive on the final colour in solid solution pigments as in mordant or heteromorphic pigments such as V–ZrO<sub>2</sub>. Therefore the obtained pigment by different methods present similar colour properties.

Finally, the Pr–Ca–cubic zirconia pigment obtained in this work is weaker yellow than V–ZrO<sub>2</sub> but the first one is less toxic (V is substituted by non-toxic praseodymium<sup>23</sup>) and more reproducible in industrial conditions than V–ZrO<sub>2</sub> due to its nature (solid solution).

#### 4. Conclusions

From the above discussion, the following conclusions may be drawn.

1. A new yellow ceramic pigment is obtained by doping Ca-cubic stabilized zirconia with praseodymium.
2. The pigment produces a soft yellow colour in ceramic glazes. the yellow colour is slightly modified by the Ca content:  $a^*$  (yellow) increases but also  $b^*$  (red) and  $L^*$ .
3. The pigment is associated to a Pr–Ca–cubic zirconia solid solution as indicated by lattice parameters, XRD and SEM-EDX analysis.

4. Sol-gel methods decrease substantially (300 °C) the pigment formation temperature in relation to that of the ceramic route.

5. Yellow pigment is obtained independently of synthesis route although each method present microstructural and crystallization differences. These facts are in agreement with the solid solution nature of the new yellow pigment.

#### Acknowledgements

The authors gratefully acknowledge the financial support of spanish CICYT (Project MAT98–0392).

#### References

1. Eppler, R. A. and Douglas Eppler, R., Which colors can and cannot be produced in ceramic glazes. *Ceram. Eng. Sci. Proc.*, 1994, **15**(1), 281–288.
2. Ray, E. H., Carnahan, T. D. and Sullivan, R. M., Tin-vanadium yellows and praseodymium yellows. *Am. Ceram. Soc. Bull.*, 1961, **40**(1), 13–16.
3. Richard Eppler, A., Zirconia-based colors for ceramic glazes. *Am. Ceram. Soc. Bull.*, 1977, **56**(2), 213–215.
4. Seabright, C. A. and Draker, H. C., Ceramic stains from zirconium and vanadium oxides. *Am. Ceram. Soc. Bull.*, 1961, **40**(1), 1–4.
5. Monrós, G., Carda, J., Tena, M. A., Escribano, P. and Alarcón, J., Synthesis of ZrO<sub>2</sub>–V<sub>2</sub>O<sub>5</sub> by sol-gel methods. *Br. Ceram. Trans. J.*, 1991, **90**, 157–160.
6. Fujiyoshi, K., Yokoyama, H., Ren, F. and Ishida, S., Chemical state of vanadium in tin-based yellow pigment. *J. Am. Ceram. Soc.*, 1993, **76**(4), 981–986.
7. Badenes, J., Cordoncillo, E., Tena, M. A., Escribano, P., Carda, J. and Monrós, G., Análisis de la variables de síntesis del pigmento

- amarillo de Pr–ZrSiO<sub>4</sub>. *Bol. Soc. Esp. Ceram. Vidr.*, 1995, **34**(3), 147–152.
8. Badenes, J. Estudio de los sistemas Pr–ZrSiO<sub>4</sub> y Pr–ZrO<sub>2</sub>. Tesis Doctoral, Universitat Jaume I, Enero 2000.
  9. Ping, Li and I-Wei, Chen., The effect of dopants on zirconia stabilization an X-ray absorption study: I, trivalent dopants. *J. Am. Ceram. Soc.*, 1991, **77**(1), 118–128.
  10. Ray, S. P. and Setubican, S. V., *Mater. Res. Bull.*, 1977, **12**, 549.
  11. Monrós, G., Carda, J., Tena, M. A., Escribano, P., Badenes, J. and Cordoncillo, E., Spinels from gelatine-protected gels. *J. Mater. Chem.*, 1995, **5**(1), 85–90.
  12. Bragg, L., *Handbook of X-Ray*. Emmett and F. Kaeble, 1967, Chapter 17, p. 1.
  13. POWCAL-LSQC Programmes, Ptt. of Chemistry, Aberdeen University UK.
  14. CIE, *Recommendations on Uniform Colour Spaces, Colour Difference Equations*. Psychometrics Colour Terms. Supplement No. 2 of CIE Publ. No. 715 (E1–131) 1971. Bureau Central de la CIE, Paris, 1978.
  15. Monrós, G., Carda, J., Tena, M. A., Escribano, P. and Alarcón, J., Effect of ZrO<sub>2</sub> precursors on the synthesis of V–ZrSiO<sub>4</sub> solid solutions by the sol-gel method. *J. Mater. Sci.*, 1992, **27**, 351–357.
  16. ASTM card No. 27–997.
  17. ASTM card No. 17–923.
  18. Garvie, R. C., Occurrence of metastable tetragonal zirconia as a crystallite size effect. *J. Phys. Chem.*, 1965, **69**(4), 1238–1243.
  19. Yashima, M., Ishizawa, N. and Yoshimura, M., Application of an iron packing model based on defect clusters to zirconia solid solutions: II, applicability of Vegard's law. *J. Am. Ceram. Soc.*, 1986, **69**(4), 325–332.
  20. Shanon, R. D., *Acta Crystallogr.*, 1976, **A32**(5), 751–767.
  21. Torres, D., Paje, S. E. and Llopis, Y. J., Coloración de monocristales de ZrO<sub>2</sub>–CaO por termoreducción. *Bol. Soc. Esp. Cerám. Vidr.*, 1995, **34**(5–6), 395–397.
  22. De, G., Licciulli, A. and Nacucchi, M., Uniformly dispersed Pr<sup>3+</sup> doped silica glass by the sol-gel process. *J. Non-Crystalline Solids*, 1996, **201**, 153–158.
  23. Windholtz, M., *The Merck Index*, 9th ed. Merck, Rahway, NJ, 1976 pp. 29–32.